Radar Signatures of Tropical Cyclone Tornadoes in Central North Carolina

DOUGLAS SCHNEIDER

National Weather Service Forecast Office, Morristown, Tennessee

SCOTT SHARP

National Weather Service Forecast Office, Raleigh, North Carolina

(Manuscript received 1 February 2006, in final form 10 August 2006)

ABSTRACT

During the tropical cyclone season of 2004, there were four tropical cyclones that spawned tornadoes in central North Carolina: Frances, Gaston, Ivan, and Jeanne. This study examines the environmental characteristics and radar signatures from these events. The tornado warning decision-making process is a difficult one during any severe weather event, but it is even more difficult in a tropical cyclone environment because of the subtlety of features and rapid tornadogenesis that can occur. Previous studies that have examined the characteristics of a tropical cyclone environment found that high low-level moisture content, high shear, and a midlevel intrusion of dry air are favorable for tornadoes. The tropical cyclones that are examined in the current study all exhibited these characteristics. Radar signatures associated with these tornadoes were more subtle and weaker when compared with nontropical cyclone tornadoes, but were still discernable. This study analyzed the radar signatures from tornadic and nontornadic storms in a tropical cyclone environment with the purpose of determining the best indicators of tornadogenesis. Three precursors were found to give good lead time for tornado touchdowns: 1) a near gate-to-gate mesocyclone rotational velocity of 20 kt (10.3 m s^{-1}) or greater, 2) a hook or appendage signature in the reflectivity data, and 3) the presence of a velocity enhancement signature of 30 kt (15.4 m s^{-1}) or greater between 7000 ft (2.1 km) and 14 000 ft (4.2 km) AGL. Using these signatures together in the tornado warning decision-making process can increase lead time and accuracy in the tropical cyclone environment.

1. Introduction

The 2004 tropical cyclone season was one of the most active on record for central North Carolina. Seven tropical cyclones impacted the area between July and September: Alex, Bonnie, Charley, Frances, Gaston, Ivan, and Jeanne. Of these seven, four were responsible for producing tornadoes in the Raleigh, North Carolina, county warning area (CWA): Frances, Gaston, Ivan, and Jeanne. There were 15 total confirmed tornadoes associated with these four tropical cyclones. This research reviewed these tornado events, with the purpose of determining the best Doppler radar warning thresholds for tornadoes in a tropical cyclone environment. By reviewing these cases, it is intended that tornado warning "best practices" be developed.

Corresponding author address: Douglas Schneider, 5974 Commerce Blvd., Morristown, TN 37814.
E-mail: douglas.schneider@noaa.gov

DOI: 10.1175/WAF992.1

a. The tropical cyclone environment

The tropical cyclone environment is very different from the typical tornadic environment. Shallow supercells are possible in tropical cyclones due to strong lower-tropospheric vertical shear, even though buoyancy is limited because ambient lapse rates are close to moist adiabatic (McCaul and Weisman 1996). McCaul (1991) described the favorable conditions for tornadoes in a tropical cyclone environment. Table 1 lists parameters and their thresholds that can be used to distinguish between a high tornado threat and a low tornado threat in a tropical cyclone environment.

Of the four tropical cyclones that produced tornadoes in central North Carolina in 2004, only one, Gaston, made direct landfall in the Carolinas. The other three made landfall either in Florida or recurved northeast after making landfall along the Gulf of Mexico coast. This placed central North Carolina in the most favorable region of a tropical cyclone for tornadoes, which is the northern to eastern quadrants between 0°

TABLE 1. Parameters that can be used to determine if a tropical cyclone environment poses a low threat or high threat of tornadoes. Adapted from McCaul (1991).

Parameter	Low threat	High threat
Location with respect to tropical cyclone's (TC's) motion direction	120°–359°	0°–120°
Lifted index (surface-based parcel)	>-1	<-2
CAPE (surface-based parcel)	<500 J kg^{-1}	>500 J kg^{-1}
0–3-km shear	<20 m s^{-1} (39 kt)	>20 m s^{-1} (39 kt)
0–1 km storm-relative helicity	<100 m^2 s^{-2}	>100 m^2 s^{-2}
Bulk Richardson number	<10 or >50	10–50
850-mb wind speed	<15 m s^{-1} (30 kt)	>15 m s^{-1} (30 kt)
Storm motion	<10 mi h^{-1} (4 m s^{-1}) or >30 mi h^{-1} (13 m s^{-1})	10 mi h^{-1} (4 m s^{-1}) to 30 mi h^{-1} (13 m s^{-1})
Axis of low-level convergence over area	No	Yes

and 120° with respect to the tropical cyclone's motion. In this quadrant, 0–3-km shear and 0–1-km storm-relative helicity are usually highest (McCaul 1991). The storm environment associated with the four tropical cyclones that were investigated in this study exhibited values that were mainly in the high threat category in Table 1.

More recent studies have shown that a low lifted condensation level (LCL) and a small surface dewpoint depression indicate an environment that is favorable for tornadoes. Studies by Markowski et al. (2002) and Thompson et al. (2003) found that increased low-level relative humidity may contribute to increased buoyancy in the rear-flank downdraft, and an increased probability of tornadoes. Simulations of storm structure by McCaul and Cohen (2002) found that a lowered LCL reduced the strength of the surface outflow, prevented outflow dominance, and promoted storm persistence. The LCL height was found to be a strong discriminator between tornadic and nontornadic supercells by Rasmussen and Blanchard (1998). LCL heights below 800 m were associated with tornadic environments 50% of the time in that study. According to Markowski et al. (2002), the mean surface dewpoint depression in tornadic environments was 10°F (5.6 K). In a tropical cyclone environment, the boundary layer relative humidity is typically high, and thus the LCL height and surface dewpoint depressions are typically low. These conditions, along with strong low-level wind shear and sufficient buoyancy, will create an environment favorable for tornadogenesis. It is uncertain whether the critical values of LCL height and surface dewpoint depression in the Great Plains studies by Rasmussen and Blanchard (1998) and Markowski et al. (2002) will differ significantly in the tropical cyclone environment; however, this is beyond the scope of this study and should be addressed in future research. LCL height and surface dewpoint depression could be added to the research by McCaul (1991) to further aid in distinguishing between a low tornado threat and a high tornado threat in the tropical cyclone environment.

Midlevel dry intrusions have been recognized as having an important impact on the tropical cyclone environment. Midlevel dry intrusions can increase convective instability by increasing the environmental lapse rate, enhancing CAPE and surface-based instability, and enhancing evaporative cooling within the rear-flank downdraft (Vescio et al. 1996). The lack of midlevel clouds due to the dry-air intrusion tends to increase diurnal heating and thus surface-based destabilization. Curtis (2004) examined 13 historical tornado outbreaks associated with tropical cyclones. A midlevel dry intrusion was identified with 11 of the outbreaks. The study found that tropical cyclones associated with tornado outbreaks and midlevel dry intrusions had a lower average LCL, had more moisture in the layer from just above the surface through 900 mb, and were much drier at heights above 700 mb than tropical cyclones that did not produce outbreaks. Dry-air intrusions appeared to have played a significant role in the 2004 tropical cyclones that affected central North Carolina. Because three of the four tornado-producing tropical cyclones made landfall along the Gulf of Mexico coast, there was ample time for a drier continental air mass to become entrained into the tropical cyclones before reaching North Carolina. This entrainment of dry air into the tropical cyclone reduced the cloud cover and allowed for greater diurnal heating and surface-based destabilization. Analysis of satellite and upper-air data indicates that all four of the tropical cyclones examined in this study exhibited some degree of dry-air intrusion. Figure 1 is a water vapor image as the remnants of Hurricane Ivan crossed the Raleigh CWA, with 500-mb upper-air data plotted. This image was taken around 1200 UTC 17 September 2004, about 3 h before the time of a tornado touchdown in the north-

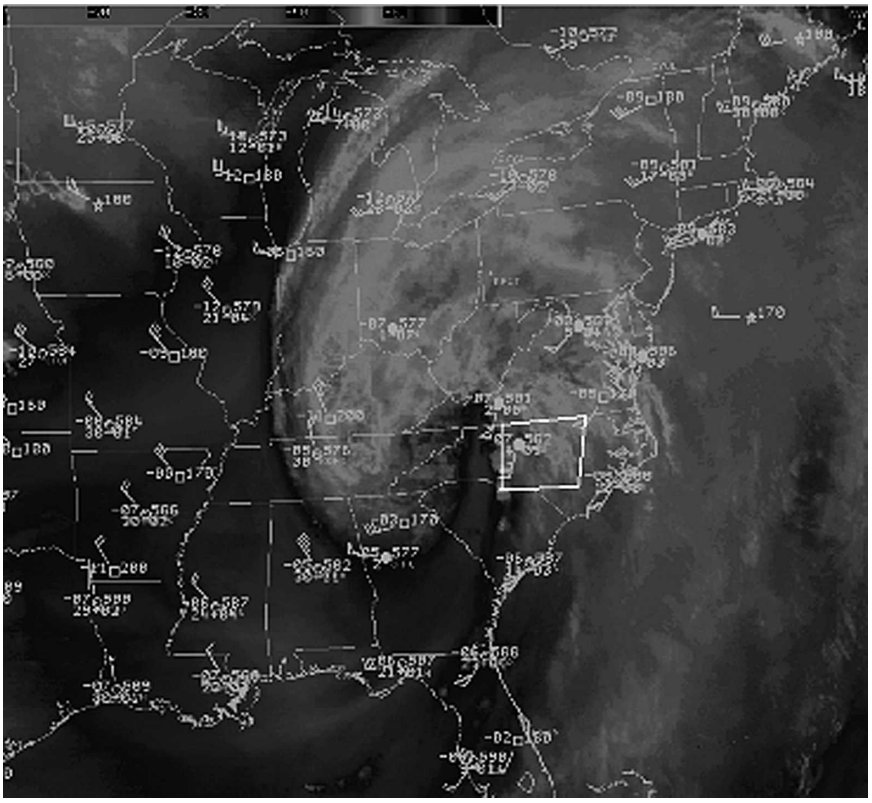

FIG. 1. Water vapor satellite imagery of the remnants of Hurricane Ivan at 1200 UTC 17 Sep 2004, with a 500-mb upper-air data plot. The center of Ivan's circulation is located about 35 mi (56 km) NW of Asheville, NC. The Raleigh CWA is indicated by the white box over central NC. A dry intrusion extends from southern GA through western NC. The 500-mb dewpoint depressions (the lower-left number in the data plots) indicate a strong moisture gradient from central NC to central TN, with dry air feeding into the circulation from AL and northern FL. At the time of this image, convection is beginning to develop along the eastern edge of the dry intrusion in NC, and a tornado was reported in the northwest portion of the Raleigh CWA about 3 h later.

west corner of the Raleigh CWA. A line of convection developed on the eastern edge of the dry intrusion, and several storms within this line produced tornadoes or straight-line wind damage as they crossed the Raleigh CWA. This dry intrusion pattern was also evident in the other three tropical cyclones that were examined in this study. The tropical cyclones in which the dry-air intrusions were most pronounced (Ivan and Jeanne) coincided with the most severe occurrences of damage.

Figure 2 is a skew *T* plot of temperature, dewpoint temperature, and winds at 1800 UTC 17 September 2004 during Ivan at Greensboro, North Carolina (GSO). The features of this sounding are very similar to the features noted by Curtis (2004) that distinguish a tropical cyclone environment that is favorable for tornadoes. The sounding from Ivan features a low LCL, saturation in the layer from just above the surface through 900 mb, and dry air at heights above 700 mb. This sounding also shows winds rapidly veering just above the surface, creating a favorable low-level shear profile for tornado formation.

Curtis (2004) also found a strong diurnal signal in the temporal distribution of the tornadoes, with 65% of the tornadoes occurring in the daylight hours. In the current study, all but one of the tornadoes examined occurred during the daylight or early evening hours between 1500 and 0000 UTC. The lack of cloud cover due to the dry intrusions along with surface heating during the day likely increased the CAPE, contributing to an enhanced tornado threat over central North Carolina during the events in this study.

The presence of low-level boundaries has been recognized as an important contributor to tornadogenesis. Although the tropical cyclone environment is often barotropic, tropical cyclones that have made landfall or are undergoing an extratropical transition can contain temperature and moisture discontinuities or wind

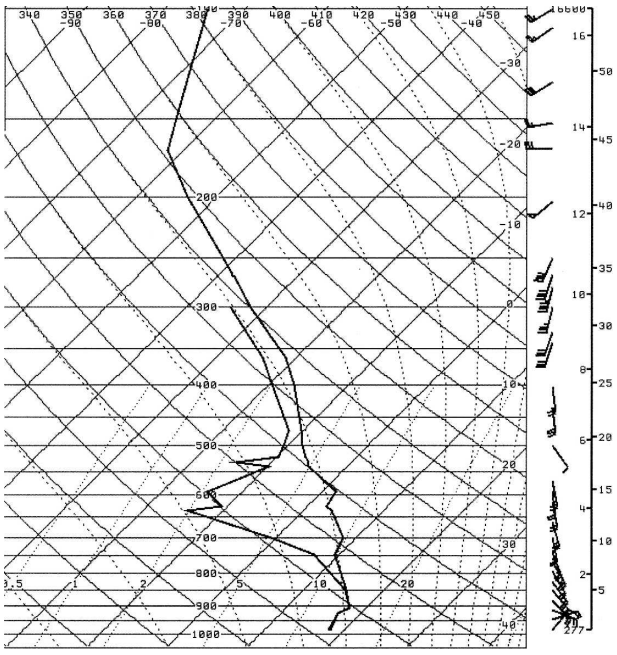

FIG. 2. A skew *T* plot of temperature, dewpoint temperature, and winds from GSO at 1800 UTC 17 Sep 2004 as the remnants of Ivan were crossing central NC. On the right side of the image is a vertical scale with km plotted on the left and thousands of ft plotted on the right. Note the low-level saturation and dry layer between 3 and 6 km, as well as the rapid veering of winds just above the surface.

convergence zones. These boundaries can locally enhance storm-relative helicity, creating a favored area for tornadoes to develop. McCaul et al. (2004) described the importance of a low-level boundary in the tornado outbreak as the remnants of Tropical Storm Beryl crossed South Carolina. In Beryl, most of the tornadoes occurred near or just northwest of a boundary, in slightly cooler surface air with backed surface winds. The presence of boundaries also played an important role in the development of several tornadoes in the current study. A boundary was present across the southern portion of the Raleigh CWA as the remnants of Hurricane Jeanne passed through the area. Numerous cells were translating from south to north, and as they encountered the east–west-oriented boundary, they produced several tornadoes. Boundaries were also present to some extent in Frances, Gaston, and Ivan as well. Knowledge of low-level boundaries can enhance the situational awareness of the warning forecaster, and potentially increase warning lead time and accuracy.

b. Structural characteristics of tropical cyclone supercells

McCaul and Weisman (1996) numerically simulated supercells within tropical cyclone environments. The simulations revealed that even though buoyancy is limited due to lapse rates that are nearly moist adiabatic, shallow supercells are still possible. These shallow supercells may contain updrafts that rival or exceed the intensity of Great Plains supercells. The simulated supercells in the study were low topped, exhibiting a reduction of horizontal and vertical size when compared with the Great Plains supercells. McCaul and Weisman (1996) found that even though parcel buoyancy is often small in tropical cyclone environments, the concentration of the buoyancy in the strongly sheared lower troposphere allows for the development of a perturbation pressure minimum that is similar to those seen in simulated Great Plains supercells. The upward dynamic pressure gradient force contributes much more [at least three times as much according to McCaul and Weisman (1996)] to the updraft speed than does buoyancy in a tropical cyclone–induced supercell. The study also found that peak updraft intensity generally occurs at low levels, usually around 6600 ft (2 km) above the surface.

In the 2004 tropical cyclones that are examined in the current study, the enhanced destabilization from the midlevel dry-air intrusion likely resulted in a greater contribution of buoyancy to the updraft strength than would have occurred without the dry-air intrusion.

c. Radar characteristics of tropical cyclone tornadoes

Previous studies have investigated the characteristics of tropical cyclone tornadoes using Weather Surveillance Radar-1988 Doppler (WSR-88D) data. McCaul et al. (2004) analyzed a severe outbreak of tornadoes associated with Tropical Storm Beryl (1994). The study observed long-lived supercells that contained well-defined mesocyclones in the velocity field, along with hook echoes on their southeastern flanks. The dimensions of the mesocyclones analyzed in that study were considerably smaller than tornadic supercells in the Great Plains. Characteristic rotational velocities in the study were in the 19–29-kt (10–15 m s^{-1}) range, occasionally reaching 39–49 kt (20–25 m s^{-1}). However, the authors acknowledge that the supercells analyzed within Beryl were probably near the top of the spectrum of tropical cyclone convective cell intensity. Given the smaller dimensions and lower rotational velocities of mesocyclones in the tropical cyclone environment, the techniques that are used to warn for non–tropical cyclone tornadoes may not apply in the tropical cyclone environment. Thresholds of rotational velocity would have to be lowered, and reflectivity signatures would be more subtle. In addition, radar sampling limitations may also lead to lower radial velocity values. Reduced

radar resolution due to the smaller storm dimensions may also contribute to lower apparent radial velocity values, especially at far distances from the radar.

In the current study, this was indeed found to be the case with most of the tornadic cells that were analyzed. Rotational velocity values were lower and reflectivity signatures were less distinct when compared with non–tropical cyclone tornado signatures. In the current study, there were a few long-lived supercells that produced multiple tornadoes, but this was the exception rather than the rule. Most of the tornadic storms observed in central North Carolina in 2004 had shallow rotation, often observed only in the lowest one or two radar elevation angles, and usually extending no higher than 15 000 ft (4.5 km). A deep persistent mesocyclone often did not precede tornado touchdown. Most of the tornadoes were very short lived with rotation signatures often lasting only two to four volume scans (about 10–20 min), much shorter than those observed in McCaul et al. (2004). However, the rotational velocity values typical of tornadic supercells in McCaul et al. (2004) [19–29 kt (10–15 m s^{-1})] were comparable to those found in this study.

Spratt et al. (1997) investigated radar signatures from several tornadic storms that occurred during Tropical Storm Gordon (1994) and Hurricane Allison (1995). Although reflectivity features such as inflow notches and hooks were more subtle, these traditional severe weather indicators were occasionally observed during several of the Gordon and Allison tornado events. Values of rotational velocity that were observed in mesocyclones in that study were in the 13–23-kt (7–12 m s^{-1}) range. This threshold value agrees closely with the findings of McCaul et al. (2004), as well as with the findings of the current study. Spratt et al. (1997) also analyzed the echo-top product, and found that trends of decreasing echo tops corresponded with a time period when the depths of the rotational velocities were determined to be increasing. The current study also examined the potential to use echo tops to predict the onset of tornadogenesis. Typical echo-top values analyzed with the storms that produced tornadoes were between 25 000 and 45 000 ft (7.6 and 13.7 km). However, with most of the storms there appeared to be no discernable pattern to the echo tops before, during, or after tornado touchdown.

2. Methodology

The Weather Event Simulator was used to review the tropical cyclone tornadoes that occurred during 2004 in association with Gaston, Frances, Ivan, and Jeanne. There were two tornadoes that occurred ahead of the remnants of Tropical Storm Bonnie that are not included in this study. While the presence of Bonnie off the south Atlantic coast likely affected the near-storm environment over central North Carolina to some degree, the thunderstorms were primarily associated with a cold front well in advance of the tropical cyclone.

Table 2 lists the cells that were examined in this study. There were 20 cells analyzed, 12 of which produced at least one tornado. There were a total of 15 separate tornado touchdowns reported. The rotational velocity (Vr) of the storm-relative velocity at 0.5° was calculated for each cell. The rotational velocity was computed by taking one-half of the absolute value of the difference between the maximum inbound velocity and the maximum outbound velocity. Though there may be inaccuracies in the rotational velocity estimation due to radar range, this method was chosen because it can be quickly calculated in an operational setting using the Advanced Weather Interactive Processing System, which is the primary tool of radar data investigation at National Weather Service offices. Higher-elevation angles of storm-relative velocity data were also analyzed. Reflectivity signatures such as hooks or appendages that may be indicative of a tornado were noted. For comparison, 13 storms that did not produce tornadoes were also analyzed. The primary WSR-88D radar used was that in Raleigh–Durham, North Carolina (KRAX), located near the center of the Raleigh CWA. It is the radar that provides the most complete coverage of the Raleigh CWA. Neighboring radars were also analyzed when the storms were near the CWA borders. An outline of the Raleigh CWA, which covers central North Carolina, can be seen in Fig. 1.

3. Results

a. Rotational velocity

All 12 cells that produced tornadoes had parent circulations with at least 15-kt (7.7 m s^{-1}) rotational velocity and less than 3 n mi diameter calculated at the 0.5° elevation angle. The average lead time from the first appearance of this threshold to the tornado touchdown was 28.5 min. However, there were eight cells that had a Vr of 15 kt (7.7 m s^{-1}) but did not produce a tornado. Using this threshold alone would produce a high probability of detection, but also a high rate of false alarms.

Raising the Vr to 20 kt (10.3 m s^{-1}) with less than 3 n mi diameter resulted in an average lead time of 25 min, with 10 detections, six false alarms, and two missed events when viewing the storms from the KRAX radar. It is important to examine these two missed events

TABLE 2. Cells that were examined in the study with a mesocyclone diameter of 3 n mi (5.5 km) or less. Listed in the table are the date of occurrence and associated tropical cyclone; the time of the first appearance of a 15-kt Vr, a 20-kt Vr, a reflectivity hook, and VES of 30 kt or greater; the maximum Vr observed and the time of occurrence; and the time of tornado touchdowns. All times are in UTC. The Vr units are kt.

Cell No.	Date and associated TC	Time of 15-kt Vr	Time of 20-kt Vr	Time of hook	Time of VES	Max Vr	Time of max Vr	Time of tornado
1	29 Aug, Gaston	1614	1704	1614	1614	21.5	1704	None
2	29 Aug, Gaston	1635	None	1630	1635	19	1645	1645
3	29 Aug, Gaston	1847	1856	None	1847	26.5	1909	1925
4	7 Sep, Frances	1851	1900	None	1932	22	1900	None
5	7 Sep, Frances	1820	None	None	None	18.5	1825	1824
6	7 Sep, Frances	1907	1912	1912	1907	21.5	1917	1956
7	8 Sep, Frances	815	836	847	836	24	847	855
8	8 Sep, Frances	1454	1509	1459	1454	26	1520	1525
9	8 Sep, Frances	1520	1530	None	1541	20	1530	None
10	8 Sep, Frances	1608	1619	1624	1613	23	1629	1645
11	17 Sep, Ivan	1435	1435	None	1435	32.5	1507	1509
12	17 Sep, Ivan	1631	1631	1636	1631	27.5	1641	1655, 1725
13	17 Sep, Ivan	1826	1826	1826	1831	27	1847	None
14	27 Sep, Jeanne	2057	2108	None	None	22	2108	None
15	27 Sep, Jeanne	2113	2129	2145	2118	40.5	2145	2141, 2220
16	27 Sep, Jeanne	2145	2145	None	None	22	2155	None
17	27 Sep, Jeanne	2258	2258	2258	2303	27.5	2330	2330
18	27 Sep, Jeanne	2330	2330	2340	2335	32.5	2356	2345, 0010
19	28 Sep, Jeanne	238	None	None	None	17.5	250	None
20	28 Sep, Jeanne	651	None	None	651	19	651	None

more closely. One of the missed tornadoes occurred in Anson County, which is located in the far southwest corner of the Raleigh CWA (cell 5 in Table 2). At a distance of 90 n mi (167 km), the lowest that KRAX can sample a cell is around 10 000 ft (3.1 km) AGL. The maximum computed Vr from KRAX with this cell before tornado touchdown was 15 kt (7.7 m s^{-1}). The radar that was able to sample the cell the lowest was in Columbia, South Carolina, around 7500 ft (2.3 km) AGL. From this radar, the Vr was calculated to be 25 kt (12.9 m s^{-1}). In this particular tornado event, it is clear that data from neighboring radars are of critical importance to obtaining the best velocity sampling possible. Other cells that were analyzed had circulations that were confined mainly to the lowest levels of the storms, usually extending no higher than 15 000 ft (4.5 km).

The second missed event was a tornado that touched down in Harnett County, about 32 n mi (60 km) southwest of KRAX (cell 2 in Table 2). The maximum Vr that was computed with this cell before the tornado touchdown was 19 kt (9.8 m s^{-1}). Figure 3 shows the 0.5° storm-relative velocity image about 10 min before tornado touchdown. Range folding in the velocity data may also have influenced the Vr calculation. However, this cell exhibited a distinct hook signature in the reflectivity data 10 min before the tornado event. Figure 4 shows the reflectivity image at the same time as the storm-relative velocity image in Fig. 3. This event stresses the need to consider multiple datasets in the warning decision-making process, and not focus on one threshold that must be met before issuing a warning. Both storm-relative velocity and reflectivity data must be examined closely to make a fully informed warning decision.

A Vr threshold of 25 kt (12.9 m s^{-1}) or greater was observed with seven tornado events. There was one cell that met or exceeded this threshold but did not produce tornado, while five tornadoes occurred below this threshold. While this threshold produced a low false alarm rate, the probability of detection was unacceptably low.

There were five storms analyzed that exhibited a Vr of 15 kt (7.7 m s^{-1}) or higher, but their rotation was broad, greater than 3 n mi (5.5 km) diameter. These storms are not listed in Table 2. When this was observed, no tornado occurred. Only when the rotation tightened to less than 3 n mi (5.5 km) diameter did a tornado touchdown follow. This is similar to the findings of Spratt et al. (1997), where a tightening of the rotation signature was found to be a precursor of tornadogenesis.

b. Velocity signatures at higher elevation angles

Of the 15 tornado events reviewed, only 3 showed rotation at or above the 1.5° elevation angle before the tornado touchdown. Strong and deep mesocyclones

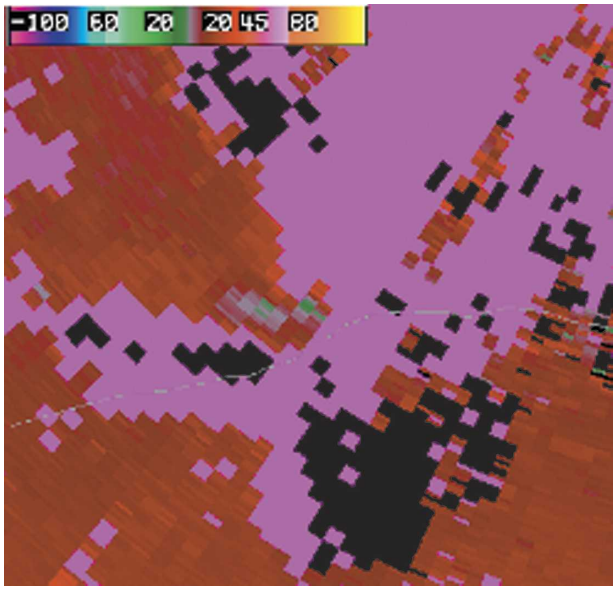

FIG. 3. The 0.5° storm-relative velocity image from KRAX at 1635 UTC 29 Aug 2004; cell 2 in Table 2. The weak rotation signature is located in the center of the image. The purple area indicates range-folded data. The KRAX radar is located just beyond the upper-right corner of the image, about 35 mi (56 km) to the NE of the rotation signature. At this distance the radar is sampling the cell around 3000 ft (900 m) AGL. Color scale units are kt.

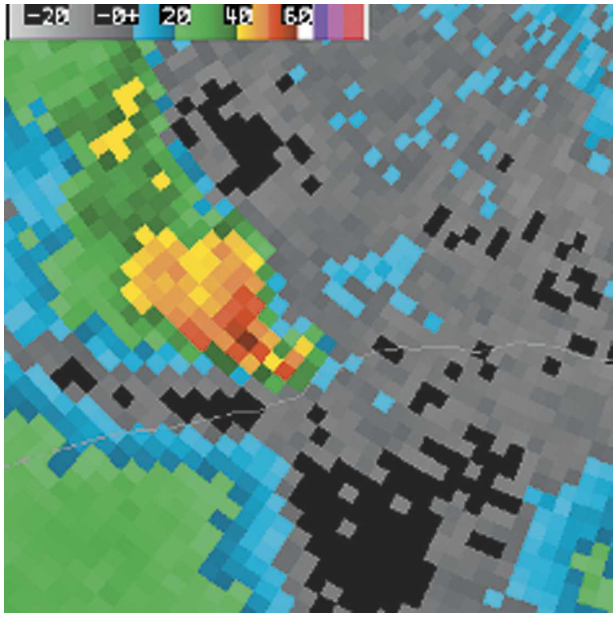

FIG. 4. The 0.5° reflectivity image from KRAX at 1635 UTC 29 Aug 2004; cell 2 in Table 2. The KRAX radar is located just beyond the upper-right corner of the image, about 35 mi (56 km) NE of the cell. The cell is being sampled by the radar around 3000 ft (900 m) AGL at this distance. Color scale units are dB*Z*.

were rarely observed in these storms. When rotation was observed aloft, it was most often broad, with the inbound and outbound velocities separated by 3 n mi (5.5 km) or greater. However, there was another signature noted at higher-elevation angles that preceded 14 tornado events. This signature will be referred to as a velocity enhancement signature (VES). This signature appeared as a small area of enhanced radial velocity of 30 kt (15.4 m s^{-1}) or greater. It was observed between 7000 (2.1 km) and 14 000 ft (4.2 km) AGL. The average lead time from the first appearance of a VES to the first tornado touchdown was 27 min, with the range of lead times from 10 to 49 min. In all of its occurrences, the VES was located above the low-level inflow region of the storm. When a VES was observed along with a hook and a low-level rotation signature, these features were vertically collocated; the VES was directly above the reflectivity hook and the low-level rotation.

There was only one tornado event that was not preceded by a VES. Thus, the VES offers a high probability of detection. There were 5 out of 12 cells that did have a VES but that did not produce tornadoes. This may suggest that the VES may also have a high false alarm rate.

Figure 5 is a storm-relative velocity image at 1.5° from cell 15 in Table 2, demonstrating the appearance of a VES. In this case, the VES appears as a small area of inbound velocities exceeding 30 kt (15.4 m s^{-1}) in northwest Hoke County. The height of this VES is about 12 500 ft (3.8 km) AGL. Figure 6 is another example of a VES, taken from the same storm at the same time as Figs. 3 and 4 (cell 2 in Table 2). In Fig. 6, the height of the VES is about 10 000 ft (3 km) AGL. A comparison of the location of the VES to the rotation in Fig. 3 and the hook signature in Fig. 4 shows that the VES is vertically collocated with these features.

The physical mechanisms within the cell that cause a VES are unclear, and should be the topic of future research. We speculate that the VES is related to the formation of the rear-flank downdraft due to its location relative to the mesocyclone and other storm signatures. It may be a storm-scale inflow jet, which is being driven by shear-induced pressure perturbations. This inflow jet may lead to or enhance the decent of the rear-flank downdraft. Whatever its cause, it is apparent that the presence of a VES can be a strong indicator of tornadogenesis, especially when observed in conjunction with reflectivity signatures and rotational velocity.

c. *Reflectivity signatures*

As was observed in the study by Spratt et al. (1997), the reflectivity signatures were more subtle than in

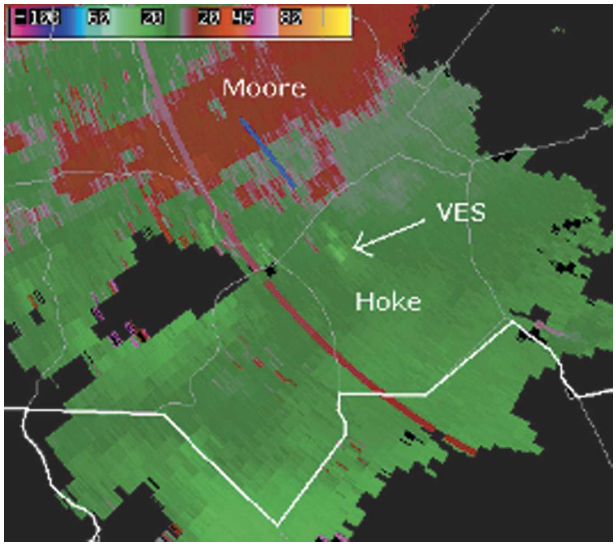

FIG. 5. The 1.5° storm-relative velocity image from KRAX at 2118 UTC 27 Sep 2004; cell 15 in Table 2. The VES is the area of inbound (green) velocities in excess of 30 kt (15.4 m s^{-1}) located in northwestern Hoke County. It preceded the tornado touchdown in southern Moore County by 23 min. The blue line indicates the approximate track of the tornado. The KRAX radar is located just beyond the upper-right corner of the image. The VES is about 62 mi (100 km) SW of the radar, which is sampling at around 12 500 ft (3800 m) AGL at this distance. Color scale units are kt.

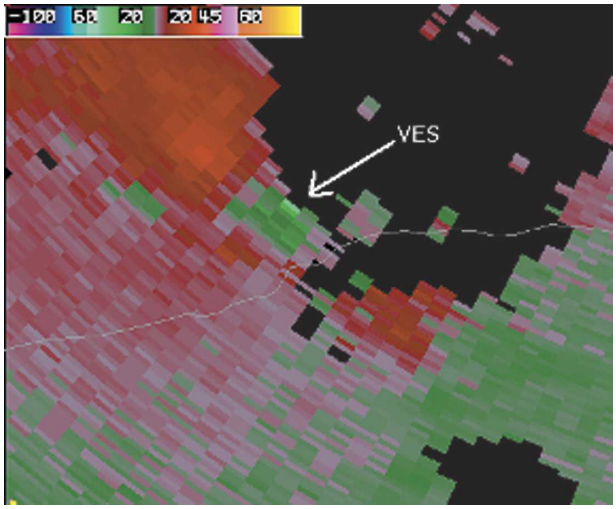

FIG. 6. The 2.4° storm-relative velocity image from KRAX at 1635 UTC 29 Aug 2004; cell 2 in Table 2, the same storm as shown in Figs. 3 and 4. A tornado touchdown occurred about 10 min after the time of this image. The VES appears as the bright inbound velocities near the center of the image. The height of the VES is about 10 000 ft (3 km) AGL. The KRAX radar is located beyond the upper-right corner of the image, about 35 mi (56 km) NE of the VES. Color scale units are kt.

non–tropical cyclone tornadoes, but they were discernable. On a few occasions, hook signatures were quite distinct, as was the case with the cell in Fig. 4. In the current study, reflectivity signatures were found to be a reliable precursor to tornado touchdown. The average lead time from the appearance of a hook or appendage to tornado touchdown was about 18 min. Of the 11 times a hook or appendage signature was present in the reflectivity data, 9 were followed by a tornado touchdown. Thus, these reflectivity signatures gave a low rate of false alarms. There were three tornadoes that touched down that were not associated with a discernable hook or appendage signature (cells 3, 5, and 11 in Table 2). An explanation for two of these missed events may be due to the far distance from the radar that the tornadoes occurred. Cells 5 and 11 occurred about 90 n mi (167 km) from the KRAX radar, and it is likely that the radar was sampling the storms well above where a hook or appendage could be seen. Cell 3 was located about 48 n mi (88.5 km), and had a maximum rotational velocity of 26.5 kt and a VES. Relying on reflectivity signatures alone would likely result in several missed tornado events, especially at far distances from the radar. The best warning decision is made when multiple signatures are considered.

4. Conclusions

The warning decision-making process is a difficult one during any severe weather event, but it is made even more difficult in a tropical cyclone environment. The high moisture and high shear of a tropical cyclone air mass can result in the quick formation of tornadoes with subtle reflectivity signatures and shallow mesocyclones. This study analyzed the radar signatures from tornadic and nontornadic storms in a tropical cyclone environment with the purpose of determining the best indicators of tornadogenesis. Three precursors were found to give good lead time for tornado touchdowns: 1) a near gate-to-gate mesocyclone rotational velocity of 20 kt (10.3 m s^{-1}) or greater, 2) a hook or appendage signature in the reflectivity data, and 3) the presence of a VES of 30 kt (15.4 m s^{-1}) or greater between 7000 (2.1 km) and 14 000 ft (4.2 km) AGL. None of these signatures should be used by themselves. All three should be considered in conjunction, along with storm environment data and other radar data, in order to make the best warning decision possible. Radar sampling limitations are also critical and need to be factored into any warning decision.

Acknowledgments. The authors thank David Hotz, Kermit Keeter, and three reviewers for helpful comments and suggestions in the preparation of this manuscript.

REFERENCES

Curtis, L., 2004: Midlevel dry intrusions as a factor in tornado outbreaks associated with landfalling tropical cyclones from the Atlantic and Gulf of Mexico. *Wea. Forecasting,* **19,** 411–427.

Markowski, P. N., J. M. Straka, and E. N. Rasmussen, 2002: Direct surface thermodynamic observations within the rear-flank downdrafts of nontornadic and tornadic supercells. *Mon. Wea. Rev.,* **130,** 1692–1721.

McCaul, E. W., Jr., 1991: Buoyancy and shear characteristics of hurricane–tornado environments. *Mon. Wea. Rev.,* **119,** 1954–1978.

——, and M. L. Weisman, 1996: Simulations of shallow supercell storms in landfalling hurricane environments. *Mon. Wea. Rev.,* **124,** 408–429.

——, and C. Cohen, 2002: The impact on simulated storm structure and intensity of variations in the mixed layer and moist layer depths. *Mon. Wea. Rev.,* **130,** 1722–1748.

——, D. E. Buechler, S. J. Goodman, and M. Cammarata, 2004: Doppler radar and lightning network observations of a severe outbreak of tropical cyclone tornadoes. *Mon. Wea. Rev.,* **132,** 1747–1763.

Rasmussen, E. N., and D. Blanchard, 1998: A baseline climatology of sounding-derived supercell and tornado forecast parameters. *Wea. Forecasting,* **13,** 1148–1164.

Spratt, S. M., D. W. Sharp, P. Welsh, A. Sandrik, F. Alsheimer, and C. Paxton, 1997: A WSR-88D assessment of tropical cyclone outer rainband tornadoes. *Wea. Forecasting,* **12,** 479–501.

Thompson, R. L., R. Edwards, J. A. Hart, K. L. Elmore, and P. Markowski, 2003: Close proximity soundings within supercell environments obtained from the Rapid Update Cycle. *Wea. Forecasting,* **18,** 1243–1261.

Vescio, M. D., S. J. Weiss, and F. P. Ostby, 1996: Tornadoes associated with Tropical Storm Beryl. *Natl. Wea. Assoc. Dig.,* **21** (1), 2–10.